Tetrahedron xxx (2017) 1–4

Contents lists available at ScienceDirect

Tetrahedron

journal homepage: www.elsevier.com/locate/tet

Visible-light fluorescence photomodulation in azo-BF_2 switches

Hai Qian [1], Baihao Shao [1], Ivan Aprahamian*

Department of Chemistry, Dartmouth College, Hanover, NH, 03755, USA

ARTICLE INFO

Article history:
Received 1 April 2017
Received in revised form
30 April 2017
Accepted 2 May 2017
Available online xxx

Keywords:
Azo-BF_2
Molecular switch
Switchable fluorescence
Visible light

ABSTRACT

Azo-BF_2 switches **1** and **2** with their extended phenanthridinyl π-system exhibit red-light fluorescence whose intensity can be photomodulated using visible-light. The *para*-methoxy group in **2** leads to a bathochromic shift in the emission band, pushing its tail further to the near infrared region. This group also changes the isomerization properties in **2**, as it does not display the concentration-dependent isomerization rate change observed in **1**, most likely because of a change in mechanism from rotation to inversion, and weaker π−π interaction in the system.

1. Introduction

Photochromic molecules that can reversibly change their fluorescence properties are of great interest in the fields of data storage,[1] biomolecule tracking,[2] super-resolution imaging,[3] among others.[4] It is envisioned that such systems can potentially be used in the non-destructive readout of stored information, enable non-intrusive *in situ* visualization of biomolecules, and augment temporal and spatial resolution by restricting diffraction effects.[5] In this respect, photoactivated green fluorescent proteins (GFP)[6] and diarylethene derivatives[7] have garnered most attention for their promising photophysical features, such as high fluorescence quantum yields and photoconversions, visible to near-infrared (NIR) light emission, and photoswitchable fluorescence responses.

The fluorescence emission in these systems, which ranges from far-ultraviolet (UV) to the near-infrared region, mostly relies on UV light excitation. This adds some limitations to the application of the fluorophores, because UV light can be easily scattered,[8] causes apoptosis, and has poor tissue and substrate penetration.[9] Consequently, there are advantages to shifting the activation wavelength of photochromic compounds in general,[10] and switches that can photomodulate emission in particular, to the visible or even NIR region of the electromagnetic spectrum.

We have previously reported on a family of azo-BF_2 complexes that can be directly photoswitched using visible[11] and NIR light sources.[12] More recently, we demonstrated that expanding the π-system in the azo-BF_2 switch from a quinolinyl to a phenanthridinyl ring (**1**) leads to aggregation, the degree of which can be used in modulating (through changes in concentration) the isomerization thermal half-life of the switch.[13] As part of our ongoing studies into this system,[14] we discovered that it exhibits red-light fluorescence, the intensity of which can be photomodulated during (photo) isomerization. In an effort to further red-shift the activation and emission wavelengths of the azo-BF_2 switch, we synthesized the *para*-methoxy (*p*-OMe) derivative **2** (Scheme 1). Here we report on the photoisomerization-dependent emission properties of these two azo-BF_2 switches.

2. Results and discussion

The azo-BF_2 switch **2** was synthesized following the procedure reported for synthesizing **1** (Scheme S1).[13] In a nutshell, the hydrazone precursor of **2** was obtained through the condensation of 2-(phenanthridin-6-yl)acetonitrile with *p*-anisidine. Treating the obtained hydrazone with $BF_3 \cdot OEt_2$ in CH_2Cl_2 gave us **2** in 9% yield. This target molecule, and its precursor were fully characterized using NMR spectroscopy and mass spectrometry (Fig. S1–S6).

2.1. Switchable fluorescence study of azo-BF_2 1

The fluorescence emission of **1** was studied at low concentration (9.0×10^{-6} M, CH_2Cl_2), to ensure that it is mainly in the monomeric

* Corresponding author.
E-mail address: ivan.aprahamian@dartmouth.edu (I. Aprahamian).
[1] Both authors contributed equally to this work.

http://dx.doi.org/10.1016/j.tet.2017.05.012
0040-4020/

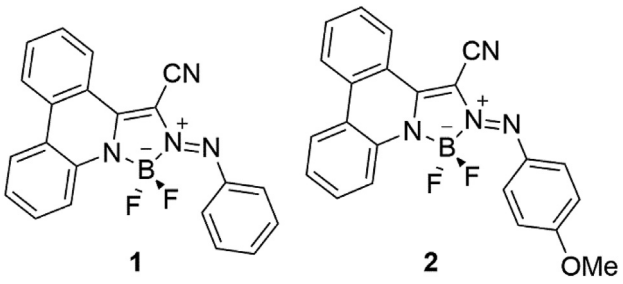

Scheme 1. Chemical structures of azo-BF_2 switches **1** and **2**.

form.[13] When excited at λ_{ex} = 508 nm,[15] **1**-*E* exhibits an intense emission band at λ_{em} = 636 nm (Fig. 1b).[16]

We speculate that the emission is stemming from the phenanthridinyl BF_2 core in **1** as the parent quinolinyl-based systems reported so far are not emissive. Upon irradiation at 600 nm, **1**-*E* isomerizes to give **1**-*Z*, accompanied with a decrease in the intensity of the red emission band.[17] The emission band reverts back to its original intensity when the solution is left to equilibrate under dark, or upon 430 nm light irradiation, which results in back isomerization. This reversible fluorescence intensity regulation can be repeated multiple times by switching the configuration of the azo-BF_2 switch **1** using visible light (Fig. 1c).

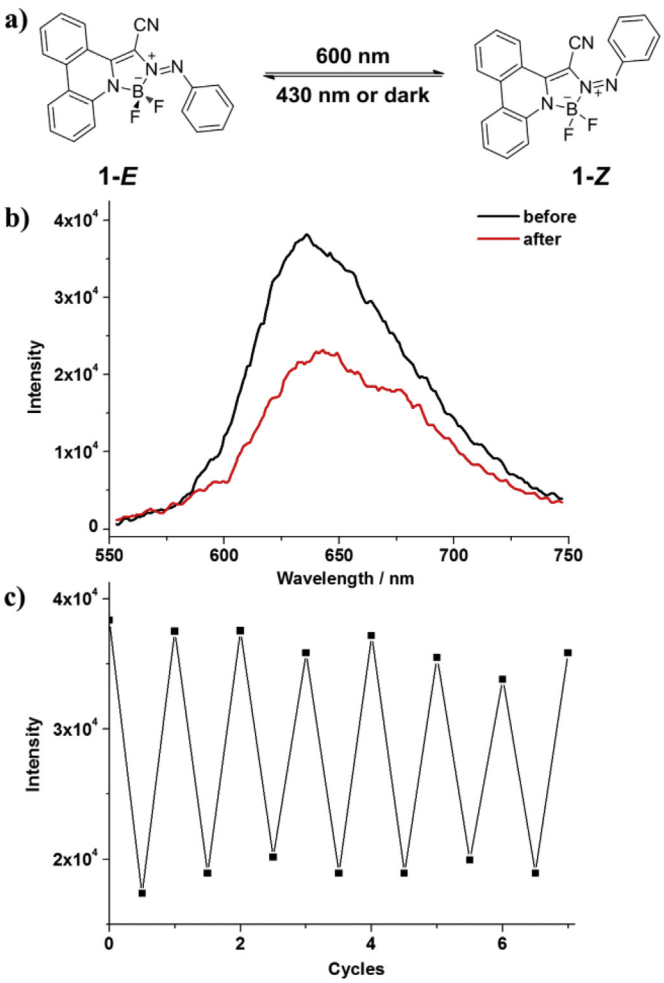

Fig. 1. (a) Visible light induced *E*/*Z* isomerization of azo-BF_2 **1**; (b) Fluorescence (λ_{ex} = 508 nm) spectra of **1**-*E* before and after irradiation with 600 nm light; (c) Isomerization cycles of **1** (9.0×10^{-6} M) in CH_2Cl_2 upon alternating irradiation using 600 and 430 nm light sources. The change in the emission intensity at λ_{max} = 636 nm was monitored.

2.2. Isomerization of azo-BF_2 2

We evaluated the photoswitching efficiency of **2** in CD_2Cl_2 using ^{1}H NMR spectroscopy. The equilibrated mixture of **2** (under dark) consists of >99% of the *E* isomer (Fig. S12a). Upon 650 nm light irradiation, the *E*-dominant sample reaches a photostationary state (PSS_{650}) consisting of 88% *Z* isomer, with a quantum yield (Φ) of 52 ± 4% (Fig. S12b). The reverse photoisomerization process ($Z \rightarrow E$) using 480 nm light irradiation yields a mixture consisting of 63% *E* isomer with $\Phi_{Z \rightarrow E}$ of 41 ± 3% (Fig. S13). Previously, we demonstrated how aggregation influences the thermal relaxation kinetics of **1**.[13] To examine whether **2** behaves similarly, concentration-dependent kinetic studies were performed. We first used dynamic light scattering (DLS) to study the aggregation behavior of **2** in solution. No DLS signals were observed at a concentration of 9.0×10^{-6} M. However, when the concentration was increased to 9.0×10^{-3} M, particles with hydrodynamic radii of 17 ± 1 nm (Fig. S14a) were detected. Irradiation of the sample with 650 nm light yields a *Z*-dominant solution, however, the particle size (18 ± 3 nm) is unaffected (Fig. S14b). The DLS data suggest that **2** might also exhibit different isomerization kinetics because of aggregation. To our surprise, the half-life does not change when going from high (1.9 ± 0.3 h), to low concentrations (1.6 ± 0.1 h) (Fig. S10–S11). An explanation to the difference in behavior between **1** and **2** might be the prevalence of inversion, rather than rotation mechanism in the *para* substituted azo-BF_2 switch, **2**. This explanation is in line with recent DFT calculations, which showed that the isomerization mechanism in the azo-BF_2 switches changes from rotation to inversion upon *para*-substitution.[18,19]

X-ray crystallographic analysis of single-crystals of **2** provided further insight into its aggregation behavior (Fig. 2). The switch adopts the *E* configuration in the solid. Each asymmetric unit contains two crystallographically independent single-crystal structures, which are distinguishable by the orientation of the *p*-OMe group (Fig. S15). More importantly, these two structures stack together in a herringbone form through a π-π interaction (3.7658(1) Å) (Fig. 2). In addition to a different packing mode (herringbone *vs.* head-to-head), the π−π interaction in **2** is weaker than in **1**, which is illustrated by the longer π−π interaction distance (3.7658(1) *vs.* 3.4956(0) and 3.4658(0) Å) and one less π interaction. This property might explain why much larger aggregates are observed in **1** than in **2** (for example 92 *vs.* 17 nm at ~9×10^{-3} M). The less compact and smaller aggregates in addition to the inversion mechanism, can together explain why the thermal isomerization rate of **2** is not affected by aggregation.

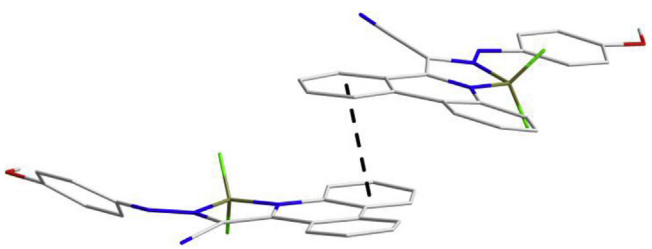

Fig. 2. Crystal packing through a π-π interaction (black dashes); the hydrogen atoms have been omitted for clarity.

Please cite this article in press as: Qian H, et al., Visible-light fluorescence photomodulation in azo-BF_2 switches, Tetrahedron (2017), http://dx.doi.org/10.1016/j.tet.2017.05.012

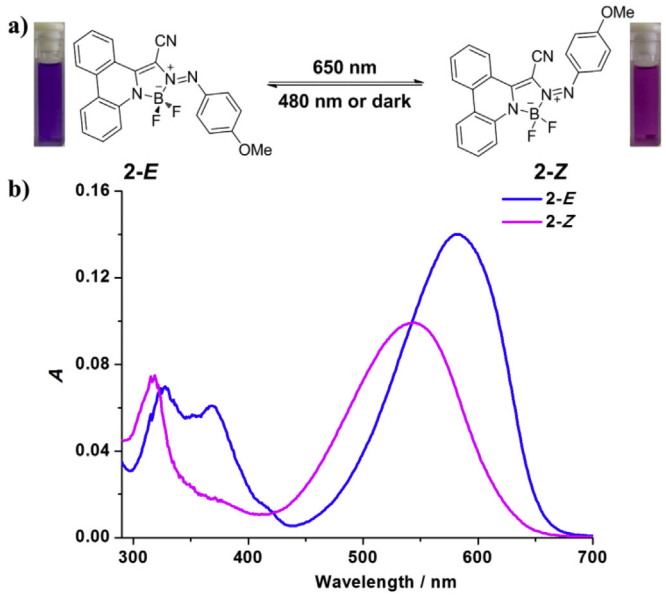

Fig. 3. (a) Visible light induced *E* (deep blue)/*Z* (purple) isomerization of azo-BF_2 **2**; (b) UV–vis spectra of **2**-*E* (deep blue) and **2**-*Z* (purple) in CH_2Cl_2 (9.0×10^{-6} M).

2.3. Fluorescence photomodulation studies

An equilibrated solution of **2** (mainly *E* form) in CH_2Cl_2 exhibits an absorption maximum (λ_{max}) at 583 nm, with an absorption coefficient constant (ε) of 15547 $M \cdot cm^{-1}$ (Fig. 3b). Upon irradiation with 650 nm light, a new absorption band arises with a $\lambda_{max} = 545$ nm, which is assigned to the *Z* isomer. This *E* to *Z* photoisomerization yields three isosbestic points at 323, 421, and 543 nm, accompanied by a significant color change of the solution from deep blue to purple. As expected, the introduction of the *para*-OMe group leads to 48 and 44 nm bathochromic shifts in the *E* and *Z* isomers, respectively, compared to the absorption maxima of non-substituted **1**.

Irradiation of **2** at $\lambda_{ex} = 543$ nm results in an emission band ($\lambda_{em} = 654$ nm) (Fig. 4a) that is red-shifted by 18 nm relative to the emission of **1**. The emission intensity decreases once **2**-*E* is isomerized to **2**-*Z* using 650 nm light irradiation. The initial fluorescence intensity cannot be restored because of the incomplete back-photoisomerization process that results in a low PSS (Fig. S13), and the relatively long thermal isomerization half-life. The reversible fluorescence switching at the PSS can be repeated multiple times upon alternating irradiation using 650 and 480 nm light sources (Fig. 4b).

3. Conclusion

Replacing the quinolinyl ring in azo-BF_2 switches with a phenanthridinyl one leads to emissive photochromic compounds whose emission can be photomodulated using visible light sources. As expected the absorption and emission bands of **2** are red-shifted relative to **1**. On the other hand, the thermal isomerization half-life of **2** is not affected by its aggregation, most likely because of a change in the isomerization mechanism to inversion, and/or formation of looser aggregates. These results indicate that the photophysical and isomerization properties of the azo-BF_2 switches are sensitive to slight structural changes. We are currently designing new azo-BF_2 derivatives with the goal of having switches with better *E*/*Z* band separations to ensure better emission photomodulation.

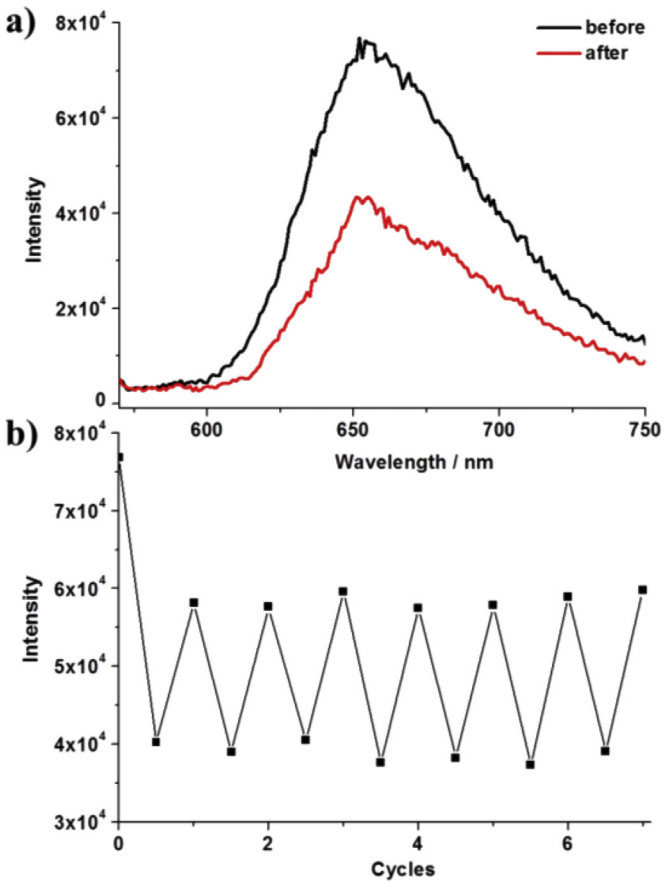

Fig. 4. (a) Fluorescence ($\lambda_{ex} = 543$ nm) spectra **2**-*E* before and after irradiation with 650 nm light; (b) Isomerization cycles of **2** (9.0×10^{-6} M) in CH_2Cl_2 upon alternating irradiation using 650 and 480 nm light sources. The change in the emission intensity at $\lambda_{max} = 654$ nm was monitored.

4. Experimental section

4.1. Synthesis and characterization of the hydrazone precursor 2-Hz

Hydrochloric acid (0.1 mL, 37%) was added dropwise to an aqueous suspension of *p*-anisidine (34 mg, 1.2 equiv, 0.28 mmol, 1 mL). After stirring at 0 °C for 30 min, a pre-cooled solution of sodium nitrite ($NaNO_2$, 1.4 equiv, 22 mg, 0.32 mmol) in 1 mL water was added dropwise to the reaction mixture over a period of 30 min, followed by 60 min stirring at 0 °C. Sodium acetate (NaOAc, 7 equiv, 131 mg, 1.6 mmol) in 1 ml water was added to a mixture of 2-(phenanthridin-6-yl)acetonitrile (50 mg, 1 equiv, 0.23 mmol) in 3 ml C_2H_5OH/CH_2Cl_2 (4:1). After stirring at r.t. for 60 min, the resulting suspension was cooled to 0 °C, followed by dropwise addition of the pre-prepared diazonium salt over a period of 20 min. The resulting reaction mixture was stirred overnight at r.t. The solution was further diluted with water (10 mL), extracted with ethyl acetate (20 × 2 mL), washed with saturated sodium bicarbonate (20 mL) and brine (30 mL), and dried over Na_2SO_4. The solvent was removed under reduced pressure and the residue was subject to silica gel column chromatography using 2:1 hexanes/dichloromethane as eluent to give **2**-Hz as a yellow solid (41 mg,

Please cite this article in press as: Qian H, et al., Visible-light fluorescence photomodulation in azo-BF_2 switches, Tetrahedron (2017), http://dx.doi.org/10.1016/j.tet.2017.05.012

51%). m.p. 191.8–192.5 °C. ^{1}H NMR (500 MHz, $CDCl_3$) δ 9.39 (d, J = 8.4 Hz, 1H), 9.14 (s, 1H), 8.72 (d, J = 8.2 Hz, 2H), 8.60 (t, J = 8.5 Hz, 2H), 8.25 (d, J = 8.0 Hz, 1H), 7.95–7.90 (m, 1H), 7.72 (dd, J = 11.1, 4.0 Hz, 1H), 7.34–7.30 (m, 2H), 7.02 (dd, J = 7.1, 5.1 Hz, 2H), 3.87 (s, 3H) ppm; ^{13}C NMR (151 MHz, $CDCl_3$) δ 149.78, 143.45, 133.91, 131.69, 130.86, 129.18, 128.00, 127.67, 123.88, 123.60, 122.59, 117.00, 115.29, 111.88, 55.83 ppm; Hi-Res MS (ESI): m/z found [M–H$^+$] for $C_{22}H_{17}N_4O^+$: 353.1397 (calcd. 353.1404).

4.2. Synthesis and characterization of **2**

2-Hz (29 mg, 0.08 mmol) was dissolved in 10 mL dry CH_2Cl_2, and the solution was transferred into a flame dried round bottom flask under N_2 gas. N,N-diisopropylethylamine (DIPEA, 7 equiv, 0.1 mL, 0.56 mmol) was added to the solution and after 2 h, BF_3•OEt_2 (10 equiv, 0.1 mL, 0.8 mmol) was added dropwise. The resulting reaction mixture was stirred under dark for 24 h. The crude mixture was concentrated under vacuum, and then subjected to silica gel column chromatography under dark using hexanes/CH_2Cl_2 (2:1 to 1:1) as eluents to give **2** as a purple solid (3 mg, 9%). m.p. 203.1–203.7 °C. ^{1}H NMR (500 MHz, CD_2Cl_2) δ 9.07 (d, J = 8.3 Hz, 1H), 8.51 (d, J = 8.4 Hz, 1H), 8.38 (d, J = 8.2 Hz, 1H), 7.94 (t, J = 7.7 Hz, 1H), 7.80 (d, J = 8.5 Hz, 1H), 7.78–7.70 (m, 3H), 7.60 (t, J = 7.8 Hz, 1H), 7.46 (t, J = 7.6 Hz, 1H), 6.98 (t, J = 6.2 Hz, 2H), 3.84 (s, 3H) ppm; ^{13}C NMR (151 MHz, CD_2Cl_2) δ 134.77, 134.54, 130.77, 128.99, 127.63, 126.52, 126.48, 126.44, 125.37, 123.21, 123.04, 121.74, 119.02, 115.15, 114.55, 55.76 ppm; ^{19}F NMR (565 MHz, CD_2Cl_2) δ −146.08 (dd, J = 65.2, 29.6 Hz) ppm. Hi-Res MS (ESI): m/z found [M–H$^+$] for $C_{22}H_{16}BF_2N_4O^+$: 401.1386 (calcd. 401.1380).

Acknowledgments

We are grateful to the Army Research Office (W911NF-15-1-0587) for the generous support. We gratefully acknowledge Prof. Richard Staples (Michigan State University) for X-ray data.

Appendix A. Supplementary data

Supplementary data related to this article can be found at http://dx.doi.org/10.1016/j.tet.2017.05.012.

References

1. Murguly E, Norsten TB, Branda NR. *Angew Chem Int Ed*. 2001;40:1752–1755.
2. Giepmans BNG, Adams SR, Ellisman MH, Tsien RY. *Science*. 2006;312:217–224.
3. Roubinet B, Bossi ML, Alt P, et al. *Angew Chem Int Ed*. 2016;55:15429–15433.
4. (a) Folling J, Belov V, Kunetsky R, et al. *Angew Chem Int Ed*. 2007;46:6266–6270;
   (b) Zacharias P, Gather MC, Kohnen A, Rehmann N, Meerholz K. *Angew Chem Int Ed*. 2009;48:4038–4041.
5. (a) Hell SW. *Science*. 2007;316:1153–1158;
   (b) Fukaminato T, Doi T, Tamaoki N, et al. *J Am Chem Soc*. 2011;133:4984–4990.
6. (a) Patterson GH, Lippincott-Schwartz J. *Science*. 2002;297:1873–1877;
   (b) Ando R, Mizuno H, Miyawaki A. *Science*. 2004;306:1370–1373.
7. (a) Irie M, Fukaminato T, Sasaki T, Tamai N, Kawai T. *Nature*. 2002;420:759–760;
   (b) Jeong YC, Yang SI, Ahn KH, Kim E. *Chem Commun*. 2005:2503–2505.
8. Beharry AA, Sadovski O, Woolley GA. *J Am Chem Soc*. 2011;133:19684–19687.
9. Wegner HA. *Angew Chem Int Ed*. 2012;51:4787–4788.
10. Siewertsen R, Neumann H, Buchheim-Stehn B, et al. *J Am Chem Soc*. 2009;131:15594–15595.
11. Yang Y, Hughes RP, Aprahamian I. *J Am Chem Soc*. 2012;134:15221–15224.
12. Yang Y, Hughes RP, Aprahamian I. *J Am Chem Soc*. 2014;136:13190–13193.
13. Qian H, Wang Y-Y, Guo D-S, Aprahamian I. *J Am Chem Soc*. 2017;139:1037–1040.
14. Qian H, Cousins ME, Horak EH, Wakefield A, Liptak MD, Aprahamian I. *Nat Chem*. 2017;9:83–87.
15. Excitation at the isosbestic point (508 nm) was chosen for the fluorescence study because it leads to minimum photoisomerization: Zhu WH, Meng XL, Yang YH, Zhang Q, Xie YS, Tian H *Chem Eur J*. 2010;16:899–906.
16. Unfortunately, the fluorescence decay lifetime was not determined because it is beyond the detection limit of our instrument (25 ps).
17. Incomplete isomerization (PSS_{600} = 91% *Z*), or a weakly emissive *Z* isomer can explain why complete quenching is not observed.
18. Wang YP, Zhang ZX, Xie M, Bai FQ, Wang PX, Zhang HX. *Dyes Pigm*. 2016;129:100–108.
19. Another indication that the isomerization mechanism might be changing in **2** is the increase in its isomerization half-life relative to **1** (hours vs seconds, respectively). Electron donating *para* substituents usually increase the thermal isomerization rate when the mechanism is rotation, which is the opposite of what we are observing for **2**.